Isotope Identification

Latimer D. Harris-Ward
Undergraduate student at the
University of the Pacific, Physics Department
(In collaboration with Kadri B. H. Nizam, Jack Lonergan, Andrew Friedman, and Savio Cao)
(Dated: September 6, 2022)

I. Introduction

Purpose

The purposes of this experimentation are as follows: (1) to confirm the reliability of the scintillator calibration factor, (2) to analyze, understand, and identify two peaks of the gamma-ray spectrum of silver, and (3) to determine the identities of two unknown radioactive sources.

The Scintillator and Background Radiation

The scintillator is comprised of two primary components: (1) the scintillation chamber and (2) the photomultiplier tube (PMT). The scintillation chamber consists of a sodium-iodide crystal, sometimes doped with thallium (NaI(Tl)). The PMT contains a photocathode, 10 dynodes, and an anode. In addition to the the scintillation chamber and the PMT, the scintillator counter is connected to a preamplifier and a multichannel analyzer (MCA). When the scintillator is used, it is important to obtain a background spectrum when analyzing data from gamma ray spectra. It is always best to take background spectra because it is unknown what forms of ionizing radiation are present during experimentation. Thus, it is always good to obtain background spectra. The background spectra is obtained in the absence of any sources. This means that the scintillator runs without any sources present; the only source of radiation is the environment surrounding the scintillator. Background spectra are used to reduce noise in the data.

The Gamma Ray Spectrum

There are various processes that dictate the production of a radionuclide's gamma ray spectrum. First, the gamma rays emitted by the source enter the scintillation chamber and collide with electrons present in the NaI(Tl) crystal. The underlying processes present when this occurs are Compton Scattering, the photoelectric effect, pair production and annihilation, and/or a combination of the preceding three effects, each with varying energies. Then, the electron passes into the PMT from the scintillation chamber and is directed through the photocathode into a focusing electrode, which sends the primary electron to the first of the ten dynodes. The dynodes serve as electron multipliers and the photocathode coupled with the anode produces a potential difference so as to generate an electric field to carry the multiplied electrons to the anode, where there is an output pulse.

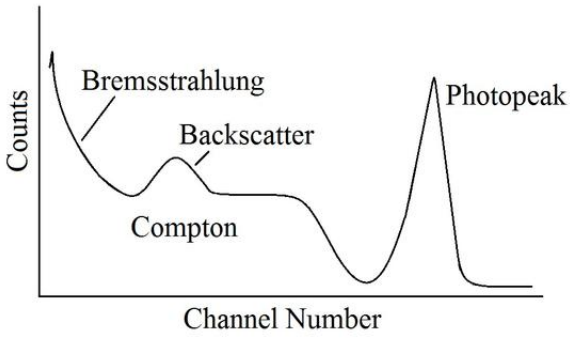

FIG. 1. The various effects present in the scintillation chamber can be seen in the gamma ray spectrum from a monoenergetic γ source.

The time between the initial electron excitation and the output pulse is called the transit time, and it is this time interval that determines the channel and the pulse height of the signal. First, The preamplifier takes weak signal inputs and outputs amplified signals that are strong enough to minimize noise and for further processing, sending them to the MCA. The MCA then takes the input signals and compartmentalizes them into different channels based on the length of the transit time, where the pulse height is proportional to the transit time. Depending on the transit time, this will determine the channel number and the pulse height, both of which produce the overall spectrum, which provides information about the different processes present. As shown in Figure 1, there are several peaks that

arise as a consequence of the different processes of the scintillator. The photopeak is produced as a result of the photoelectric effect, where the energy of the gamma ray is completely transferred to the electron in the NaI crystal. The Compton edge, the flat part of the graph, is a consequence of Compton Scattering, where not all of the energy is transferred from the gamma ray to the electron. The backscatter peak results from positron-electron annihilation. Finally, the Bremmsstrahlung ("braking radiation") portion of the spectrum arises because of the energies of decelerating electrons scattered by the gamma rays. Figure 3 shows the difference between an idealized gamma ray spectrum and a non-ideal gamma ray spectrum. For the idealized spectrum, the photopeak, the backscattered peak, and the Compton edge would have infinite resolution. However, due to the fact that other processes are present, affecting the energies of the multiplied electrons in different ways, this causes the resolution to be finite, producing spectra with distributions of counts instead of idealized spectra.

II. Data Acquisition

FIG. 2. The experimental set-up.

Materials

The materials used in the calibration, as per Figure 2, were: the SDA38 NaI(Tl) Detector, the lead shield, the 10 position sample stand, the BNC connector, the high voltage cable, the USX software, silver, an unknown disk source, an unknown rod source, and bananas.

Procedure and Methods

FIG. 3. Bananas, which were used in the experimentation.

To begin experimentation, the settings of operation were first chosen so as to provide the best resolution of the photopeak. The parameters that were chosen were the coarse gain, the fine gain, the conversion gain, the high voltage, and the preset time. The coarse gain determines how compressed or stretched out the spectrum is. The fine gain and conversion gain together determine the density of channels of the spectrum. The high voltage is used to induce a potential difference to generate an electric field, which carries the multiplied electrons to the anode, and the preset time determines the duration during which the spectrum is obtained. The coarse gain was 16, the fine gain was 1.5, the conversion gain was 1024, the high voltage was 1000 V, and the preset time was 900 seconds, using the real time instead of the live time. The reason for this distinction is because the live time depends on the dead-time and will account for the time during which the scintillator is quenched, not detecting energies. The real time measures the uninterrupted time of measurement. Afterwards, the background spectrum was taken to minimize errors due to counts. Then, the spectra of silver and both unknown sources were obtained and analyzed. Then, the calibration factor previously obtained was used to determine whether the calibration factor was dependable using Na-22, Co-60, and Cs-137. Afterwards, the calibration factor was applied to both the silver and the unknown sources so as to confirm the silver isotopes present and to determine the the identities of the unknown sources. For the bananas, a different scintillator was used with the settings for the voltage, conversion gain, fine gain, coarse gain, and real time set to be 1100 V, 4096, 1.94, 16, and 47.1 hours with a calibration factor of $y = 0.0004x + 0.0250$ with uncertainties for the

slope and y-intercept of $\pm 3 \times 10^{-8}$ and $\pm 3 \times 10^{-5}$, and y being in MeV. After the background was measured for the bananas and the gamma ray spectrum was obtained, the calibration factor was used to determine the energy of the associated channel number.

III. Data Analysis

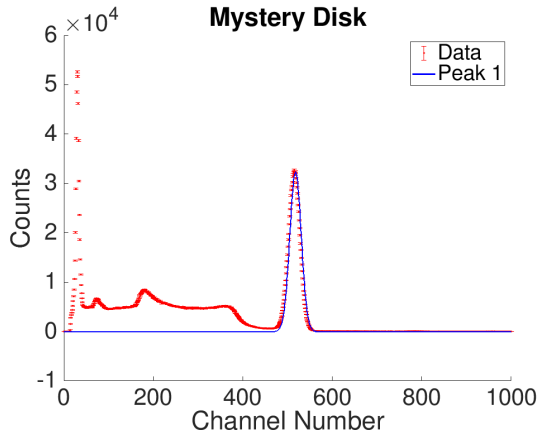

FIG. 4. The graphs of the fit for the unknown disk.

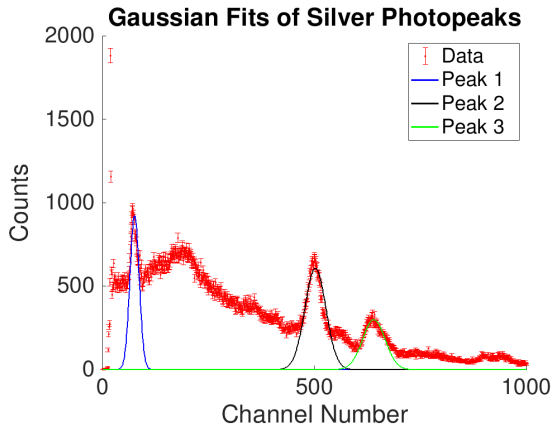

FIG. 5. The graph of the fits for the silver isotopes.

The channel numbers obtained from the spectra from the previous lab were applied to the calibration factor of $y = 614.41x + 103.42$, where the uncertainties in the slope and the y-intercept are ± 0.04 and ± 0.03, respectively. The values of the channel numbers for Na-22, Co-60, and Cs-137 were used to calculate the energies using the calibration factor, taking into account the uncertainties present in each quantity. Because count events are random and independent, and because every quantity was derived from random and independent data, the general rule of error propagation was applied so as to obtain the uncertainties in the calculated energies. The equations that were used are as follows:

$$x = \frac{y-b}{m}$$

$$\delta x = \sqrt{\left(\frac{\partial x}{\partial y}\delta y\right)^2 + \left(\frac{\partial x}{\partial m}\delta m\right)^2 + \left(\frac{\partial x}{\partial b}\delta b\right)^2}$$

$$= \sqrt{\left(\frac{\delta y}{m}\right)^2 + \left(\frac{b-y}{m^2}\delta m\right)^2 + \left(\frac{\delta b}{m}\right)^2}. \quad (1)$$

where x is the energy in Mev, y is the channel number, m is the slope of the line in channel/Mev, and b is the y-intercept in channels. Afterwards, the data for the silver and the unknown isotopes were plotted with their Gaussian fits, with the channel number on the x-axis and the number of counts on the y-axis, as shown Figures 3,4 and 5. The background spectrum was subtracted from each spectrum to reduce noise in the data and to minimize uncertainties. Then, 1000 Monte Carlo simulations were run in order to determine the mean channel number of the photopeak and the associated standard deviation, using a Gaussian model. This was done, again, due to the random and independent nature of radioactive decay events. Then, the values that were obtained were substituted into the calibration factor in order to obtain the energy and the associated uncertainty. Lastly, these calculated values were compared with the tabulated values of the energy[1] in order to determine the identity of the unknown isotopes.

In order to determine the identity of the gamma ray source present in the bananas, the calibration factor of $y = 0.0004x + 0.0250$ with uncertainties for the slope and y-intercept of $\pm(3 \times 10^{-8})$ and $\pm(3 \times 10^{-5})$, and y being in MeV. The photopeak present in the plot for the bananas was fit using 5000 Monte Carlo approximations using the Gaussian Model. After the fits were obtained for the channel number, the arithmetic mean and the standard deviation was taken of the 5000 Monte Carlo runs to obtain the best estimation of the channel number and its uncertainty. Then, the value of the channel number was used to compute the energy associated with the peak, using equation (1) to compute the

[1] https://www.nndc.bnl.gov/sigma/index.jsp?as=65&lib=endfb7.1&nsub=4

uncertainties. The plot for the gamma ray spectrum obtained from the bananas is given in Figure 7.

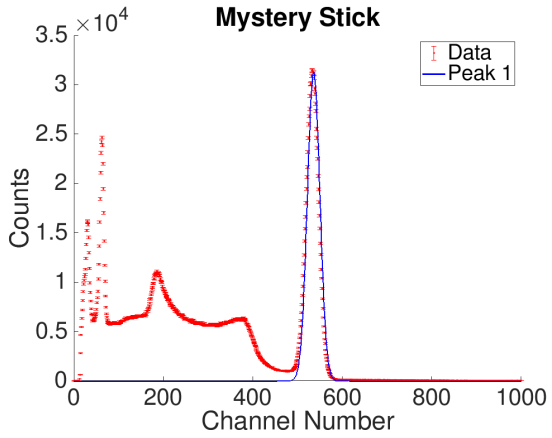

FIG. 6. The graphs of the fit for the unknown rod.

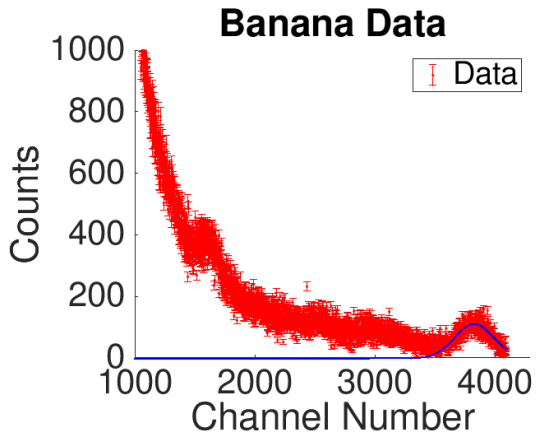

FIG. 7. The graph of the fit for the bananas.

IV. Discussion

The values of the channel numbers in the order of Na-22, Co-60, and Cs-137, going from lowest energy to highest energy, are 415.27 ± 0.01, 866.52 ± 0.04, 829.76 ± 0.04, 917.46 ± 0.03, and 511.23 ± 0.03. The calibration factor excluding the second peak for Na-22 was used because it proved to be more reliable than the calibration factor that included all of the data points. After substituting the channel numbers into the equations, the respective energies that were obtained were 0.50756 ± 0.00006, 1.1822 ± 0.0001. 1.3249 ± 0.0001, and 0.66374 ± 0.00008, all in MeV. Although it appears as though there is great precision, this is only because of the numerical prefix of "Mega," which accounts for a factor of 10^6. The values of the tabulated energies for the isotopes in the same respective order are 0.511 ± 0.013, 1.173 ± 0.004, 1.333 ± 0.005, and 0.662 ± 0.003, all in MeV. Comparatively, the Na-22 and the Cs-137 values lie within the range of the tabulated energies; however, the calculated values for both Co-60 peaks lie just outside of the range of the tabulated values. The discrepancy for the first peak is 0.009 MeV, 90 times greater than the associated uncertainty, and the discrepancy for the second peak is 0.008, which is 80 times greater than the associated uncertainty. This would suggest that the values are significantly different. Despite this, the calculated values are very close to the tabulated values, suggesting that the calibration factor is good. For the silver, the obtained channel number for the first and second peak were determined to be 500.1 ± 0.2 and 638.5 ± 0.4, respectively. After substituting these values into the calibration factor, the calculated energies were 0.6456 ± 0.0003 and 0.8705 ± 0.0007, both in MeV. The actual values for the energies were those for Ag-110 and Ag-108 with energies of 0.88026 ± 0.001 and 0.65750 ± 0.001, respectively and in MeV. Both values that were calculated do not fall within the tabulated range for both isotopes, but there is reason to believe that both Ag-110 and Ag-108 are present, due to the measured half-lives and because the actual values lie just outside of the range of the tabulated values, even though they do not lie within the error bars. For the mystery elements, the obtained channel numbers for the disk and the rod are 516.22 ± 0.02 and 534.45 ± 0.02, respectively. Further, the calculated energies are 0.67187 ± 0.00007 and 0.70154 ± 0.00007 MeV. Based on the energies, the identity of the disk is Cs-137 and the identity of the rod is Niobium-94, with energies of 0.66164 ± 0.003 and 702.639 ± 0.004 MeV, respectively[2]. The energy for the calculated Cs-137 is slightly off. Also, if the rod is Nb-94, then the calculated energy falls within the range very well.

In this experimentation, the primary sources of uncertainty were the dead time of the scintillator counter, background radiation, the natural uncertainty in the activity of the radioisotopes, and the fact that sources were unknown. The first three uncertainties have a direct effect on the number of counts observed for each channel. The dead time produces uncertainty because when the scintillator

[2] https://www.nds.iaea.org/xgamma_standards/genergiesb.htm

counter is quenched, the counter is unable to detect additional pulses; however, this effect was reduced because the real time was used instead of the live time. Of course, this is still an instrumental limitation, which will always be present. The background contributes extra counts to the data but the effects were reduced by subtracting the background from collected data. Then, because activities can not be measured precisely, there will always be a natural uncertainty with the activity of a radioisotope, which cannot be minimized. Lastly, the fact that two isotopes adds uncertainty.

The way that this experimentation could be improved is by calibrating the scintillator better. If the calibration of the scintillator had been performed more carefully, then there would be decent error bars, within which the actual values of the energies may have fallen. It is important to understand how to calibrate a scintillator because if it is not calibrated correctly, then every measurement afterwards is not reliable. The experiment could also be improved by increasing the number of channels for variability in the data and increasing the time during which the data was collected. This would ensure that peaks were more defined for better fits to the data.

For the banana data, the value obtained for the energy was 1.555 ± 0.115 MeV. Because bananas were used in the experimentation, it was natural to assume that an isotope of potassium was the gamma ray source. The isotope that was determined to be the source of gamma rays was Potassium 40, or K-40, with an energy of 1.4608 MeV. The associated discrepancy is only 0.0942 MeV, which corresponds to less than half of the uncertainty. These values for the energy obtained is consistent with the calculated value for the energy of the photopeak in the banana spectrum. This suggests that the data obtention and the data itself was adequate. Further, because the same methods of analysis were used to fit the banana data and the data for the other radioisotopes, this suggests that the data obtained for the other peaks and the calibration factor used to fit the respective data needed improvement.

V. Conclusion

In conclusion, the calibration factor of $y = 614.41x + 103.42$ was sufficient to use for determining the energies of Na-22, Co-60, Cs-137, Silver, and Nb-94. The isotopes of silver were determined to be Ag-110 and Ag-108 and the identities of the unknown disk and the unknown rod were surmised to be Cs-137 and Nb-94 due to how close to and how inside of the actual tabulated energy ranges the values were. The background is needed to reduce noise and to decrease random errors in the data. Lastly, this experimentation could be improved by bettering the calibration of the scintillator, running the experiment for longer, and increasing the number of channels. For the banana data, the value of the energy that was calculated was 1.555 ± 0.115 MeV, suggesting that the gamma source was Potassium 40 with a discrepancy of 0.0942 MeV, suggesting that the data was adequate and that improvements should be made for the former half of experimentation.

VI. References

1. https://www.nndc.bnl.gov/sigma/index.jsp?
2. https://www-nds.iaea.org/xgamma_standards